quama were unlikely to have evolved more than once. Significantly, the development of *Longisquama*'s integumentary appendages probably followed complex specialized patterns previously thought to be distinct to avian feathers. Thus, we interpret the pinnate appendages of *Longisquama* as nonavian feathers, probably homologous to those in birds.

Archaeopteryx, the earliest known bird (145 Ma), possessed a complete plumage of flight feathers that differed little from those of many extant birds (*8*, *11*). Consequently, factors associated with earlier stages of feather evolution, the morphology of the earliest feathers, and the taxonomic groups in which they first occurred remain uncertain. Nevertheless, if *Longisquama*'s integumentary appendages are homologous with those of birds, they may provide insight into an evolutionary grade through which feathers passed almost 75 million years before *Archaeopteryx* and perhaps before the origin of Aves itself.

References and Notes

1. A. G. Sharov, *Palaeontol. J.* **1**, 127, plate VIII (1970).
2. I. A. Dobruskina, *Tr. Paleontol. Inst. Acad. Nauk SSSR* **346**, 1 (1980).
3. H. Haubold and E. Buffetaut, C. *R. Acad. Sci. Paris* **305**, 65 (1987).
4. All known specimens of *L. insignis* are part of the collection of the Paleontological Institute of the Russian Academy of Sciences, Moscow (PIN). These include specimen number PIN 2584/4: the holotype specimen, slab (and counterslab) of the anterior portion of the body [see Figs. 1, 2, and 6 (right)]; PIN 2584/5: a partial single elongate integumentary appendage (no shaft base preserved) (Fig. 4); PIN 2584/6: the mid-regions of two incomplete elongate integumentary appendages; PIN 2584/7: a partial individual elongate integumentary appendage (no shaft base preserved); and PIN 2584/9: associated distal portions of approximately six incomplete elongate integumentary appendages (Fig. 5). We directly examined these specimens at the University of Kansas, Lawrence, in April 1999.
5. We interpret pinnae to have been distinct from one another, rather than merely plications on a continuous surface, for two reasons. First, the texture and color of the matrix composing the surfaces of the pinnae are qualitatively different from that of the matrix between the pinnae. In a continuous surface, matrix quality would have been more homogenous. Second, some pinnae appear to have been disturbed post-depositionally and are preserved in overlapped positions (Web fig. 2).
6. P. F. A. Maderson *et al.*, *J. Morphol.* **236**, 1 (1998).
7. F. R. Lillie and H. Wang, *Physiol. Zool.* **14**, 103, plates 1 through 8 (1941).
8. A. M. Lucas and P. R. Stettenheim, *Avian Anatomy: Integument* (Agricultural Handbook 362, U.S. Department of Agriculture, Washington, DC, 1972).
9. P. Stettenheim, in *Proceedings of the 16th International Ornithological Congress*, Canberra, Australia, August 1974, (Australian Academy of Science, Canberra City, Australia, 1976), pp. 385–401.
10. The animal apparently was preserved in a quiet lacustrine environment. Some skeletal elements were preserved, but most of the right-side elongate integumentary appendages either floated away or rotated caudally. Their preservation probably resulted from infill by fine-grained sediment. Proximally, a few of the left-side shaft bases maintained themselves as hollow tubes that eventually fractured down their centers during compaction. The outer surface of the sheath was essentially featureless, although underlying compacted structures pressed outwardly against it. In the mid-shaft region, the axis and pinnae are sharply defined in places where parts of the epidermal sheath broke away during collection of the specimen. Preservation of the axis and individual pinnae in this region is consistent with there having been enough empty space within the sheath that, when filled with fine-grained mud, the morphology of the structures within was faithfully recorded.
11. A. Feduccia, *The Origin and Evolution of Birds* (Yale Univ. Press, New Haven, CT, ed. 2, 1999).

12. We thank S. Poitras, C. Campbell, S. Olson, and the Palaeontological Institute of the Russian Academy of Sciences for assistance in procurement of specimens. T. Dujsebayeva's English translation of Sharov's original paper, photographs of modern bird feathers by A. Brower, and J. Atkinson's assistance with juvenile birds were invaluable. Supported by an NSF grant to J.A.R. and W.J.H. and by a Russian Fund for Basic Research Grant to E.N.K. and V.A.

29 March 2000; accepted 12 May 2000

A Metalloprotease Disintegrin That Controls Cell Migration in *Caenorhabditis elegans*

Kiyoji Nishiwaki,[1]* Naoki Hisamoto,[2] Kunihiro Matsumoto[2]

In *Caenorhabditis elegans*, the gonad acquires two U-shaped arms by the directed migration of its distal tip cells (DTCs) along the body wall basement membranes. Correct migration of DTCs requires the *mig-17* gene, which encodes a member of the metalloprotease-disintegrin protein family. The MIG-17 protein is secreted from muscle cells of the body wall and localizes in the basement membranes of gonad. This localization is dependent on the disintegrin-like domain of MIG-17 and its catalytic activity. These results suggest that the MIG-17 metalloprotease directs migration of DTCs by remodeling the basement membrane.

Many new insights into the molecular mechanisms controlling cell migration have been gained by the genetic analysis of model organisms such as the nematode *C. elegans*. The shape of the *C. elegans* hermaphrodite gonad is determined by the migration path of the DTCs during larval development (*1*). DTCs migrate in a complex trajectory consisting of three linear phases punctuated by two orthogonal turns (Fig. 1, A and B). DTCs are generated at the ventral midbody and migrate in opposite directions along the basement membranes of ventral body wall muscles. Mutation of the *mig-17* gene alters DTC migration (*2*): initially, migration along the ventral body wall muscles is normal, but the migration path deviates from normal after the dorsal turn (Fig. 1C). In addition, these DTCs often detach from the dorsal muscles and migrate along the intestine or gonad. As a result of this misdirected migration, *mig-17* mutants exhibit morphologically abnormal gonadal arms (*3*). These results indicate that *mig-17* is not required for DTC migration per se, but rather influences the route of migration.

A similar defect is observed in the male gonad of *mig-17* mutant worms. In wild-type worms, the male linker cell (MLC) migrates anteriorly, then reflexes and migrates to the posterior end of the worm (Fig. 1, D and E) (*1*). In *mig-17* mutants, the MLC fails to migrate correctly (Fig. 1F). However, mutation of *mig-17* does not affect the migration of other cell types such as HSN neurons and Q neuroblasts (*2*). Therefore, *mig-17* does not affect cell migration generally, but rather is required specifically for the correct migration of gonadal leader cells.

We cloned the *mig-17* gene by positional mapping followed by transformation rescue (*4*). Fragments containing only the F57B7.4 gene rescued *mig-17(k174)*. The *mig-17* gene encodes a single protein of 509 amino acids length (Fig. 2A). The MIG-17 protein is a member of the metalloprotease-disintegrin protein (ADAM) family (*5*). It contains a signal sequence followed by a pro-domain, a catalytic domain, a disintegrin-like (DI) domain, and a cysteine-rich domain (Fig. 2B). MIG-17 also lacks a transmembrane domain, suggesting that it is secreted. Comparison with the ADAM family members indicates that MIG-17 is most similar to the mouse ADAMTS-1 (*6*). The metalloprotease and DI domains are relatively well conserved (Fig. 2A). However, the domain organization in the COOH-terminal region following the DI domain of ADAMTS-1 diverges from that of MIG-17 in that ADAMTS-1 possesses the thrombospondin type I motif (*6*), whereas MIG-17 does not.

We sequenced four *mig-17* mutant alleles

[1]PRESTO, Japan Science and Technology Corporation and Fundamental Research Laboratories, NEC Corporation, Miyukigaoka, Tsukuba 305-8501, Japan. [2]Department of Molecular Biology, Graduate School of Science, Nagoya University, and CREST, Japan Science and Technology Corporation, Chikusa-ku, Nagoya 464-8602, Japan.

*To whom correspondence should be addressed. E-mail address: nishiwak@frl.cl.nec.co.jp

(*7*). The *k135* and *k174* alleles involve missense and nonsense mutations, respectively, in the pro-domain. The *k167* and *k176* mutations occurred in the metalloprotease domain (Fig. 2A). The putative metalloprotease catalytic domain of MIG-17 has a zinc-binding motif similar to the HEXXHXXGXXH motif (*5, 8*) found in the ADAM family (Fig. 2A). We examined mutant rescue by a MIG-17 transgene bearing a mutation that changes Glu^{303} to Ala (E303A) within the metalloprotease active site. In the zinc-binding metalloproteases, this mutation abolishes enzymatic activity without altering protein structure or stability (*9*). The wild-type *mig-17* was able to rescue the DTC migration defects of *mig-17(k174)* mutants, but *mig-17(E303A)* was not (Fig. 2B). We conclude that MIG-17 is an active metalloprotease and that metalloprotease activity is essential for its function in controlling DTC migration.

In addition to its metalloprotease domain, MIG-17 possesses pro-, DI, and cysteine-rich domains. To determine whether these domains are essential for DTC migration, deletion mutations lacking each domain were generated (Fig. 2B). When these transgenes were introduced into *mig-17(k174)* mutants and the rescue of DTC migration was scored, none rescued the mutant phenotypes. Thus, the pro-, DI, and cysteine-rich domains are all critical for MIG-17 activity leading to proper DTC migration.

To determine where and when MIG-17 is expressed during development, we constructed a translational fusion between *mig-17*, including the gene promoter, and the green fluorescent protein (GFP), *mig-17::GFP* (*10*). This fusion could rescue *mig-17* mutant defects (Fig. 2B), suggesting that the fusion protein was functional and expressed in all cells that require *mig-17* activity. Protein immunoblotting (*11*) identified two main bands of 105- and 70-kD size in animals expressing MIG-17::GFP (Fig. 2C). We tentatively assigned the 105-kD band as the precursor form, and the 70-kD band as the processed form generated by cleavage of the prodomain. These sizes are larger than those calculated from the primary structure and most likely reflect glycosylation of the MIG-17::GFP polypeptides. GFP fluorescence was observed on the pseudocoelomic face of body wall muscles, but not on their hypodermal face (Fig. 3, A and B). This expression pattern was first detected in late embryos and continued through the adult stage. Expression of *mig-17* was also seen on the surface of gonad, starting when the DTCs migrated over the lateral hypodermis toward the dorsal muscles (Fig. 3, C through F). This timing of *mig-17* expression on the gonad is correlated with the stage at which the DTC migration defect is first observed in *mig-17* mutants (Fig. 1C). This suggests that *mig-17* expression on the gonad is required for proper migration of DTCs.

To further examine the expression pattern of *mig-17*, we constructed another fusion gene (*mig-17ΔSP::GFP*), which lacks a predicted signal peptide of MIG-17 (Fig. 2B). Transgenic animals carrying *mig-17ΔSP::GFP* exhibited GFP fluorescence in the cytoplasm of the body wall muscle cells but not on the gonadal cells. This raises the possibility that the MIG-17 protein is produced in the body wall muscles and secreted. To test this possibility, the *unc-54* promoter (*12*) was used to express the wild-type *mig-17* fused to GFP in body wall muscles. When this *unc54p::mig-17::GFP* transgene (*10*) was introduced into *mig-17(k174)* mutant animals, it was able to rescue the DTC migration defects (Fig. 4B). Next, to examine whether expression of *mig-17* on the gonad is sufficient to direct DTC migration, we expressed *mig-17* under the control of the *lag-2* promoter (*13*), which drives expression in the hermaphrodite DTC. Transgenic *mig-17(k174)* mutants harboring the *lag-2p::mig-17::GFP* transgene (*10*) showed normal DTC migration (Fig. 4C). In these animals, GFP fluorescence was limited to the DTCs but not observed on the body wall muscles. Thus, expression of *mig-17* on the gonad is important for its effect on DTC migration. Taken together, these results suggest that MIG-17 is secreted from muscle cells and functions in the basement membrane of the gonad to guide DTC migration.

How does MIG-17 localize to the surface of the gonad after it is secreted from the body wall muscle? It is believed that the DI domains of ADAMs may mediate interactions with the extracellular matrix or cell surface receptors (*5*). Similarly, the DI domain in MIG-17 could be important for its localization. Indeed, we observed that in animals expressing the reporter construct *mig-17ΔDI::GFP*, which lacks the DI domain of MIG-17, GFP fluorescence was present on the body wall muscles but not on the surface of the gonad (Fig. 2B). Even

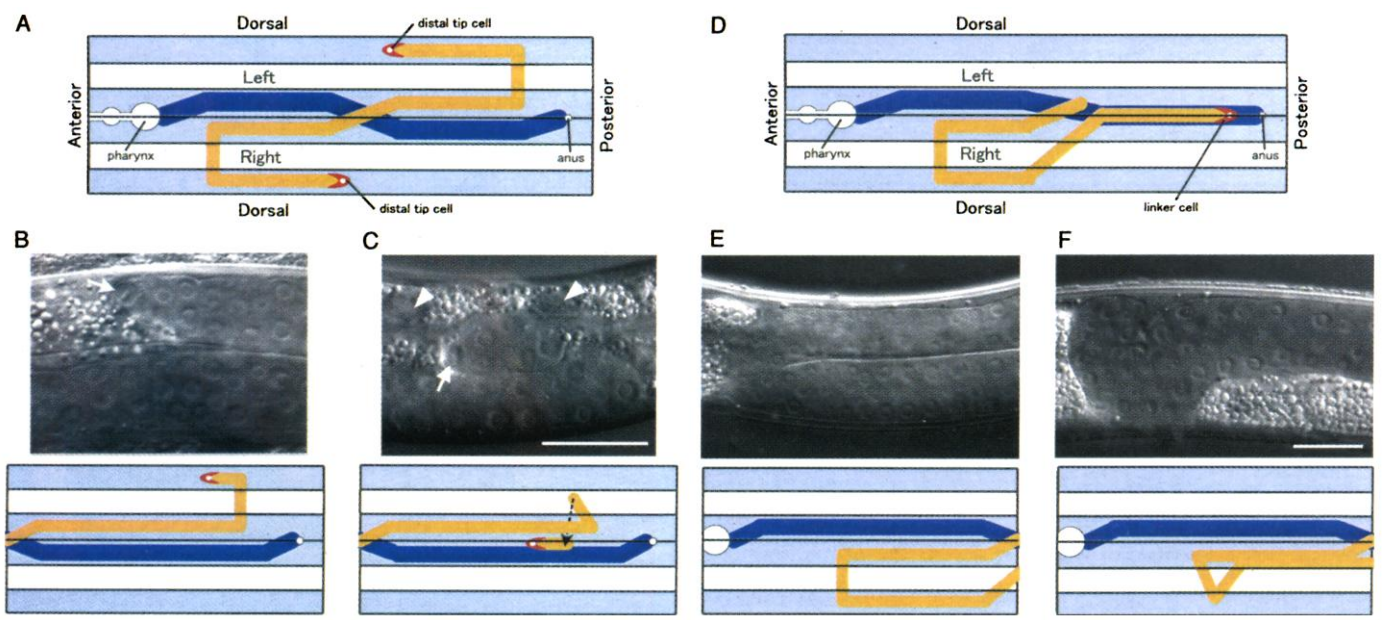

Fig. 1. Morphogenesis in *C. elegans* gonads. (**A**) DTC migration in hermaphrodites. A cylindrical projection opened along the dorsal midline. Dorsal and ventral body wall muscles, light blue; lateral epidermis, white; gonad, orange; intestine, dark blue. (**B** and **C**) DTC migration in wild-type (B) and *mig-17(K174)* (C) animals. The photos show posterior gonad arms. Anterior is left and dorsal is top. Arrows indicate DTCs. Morphology of gonadal arms is illustrated below the photo. The DTC and the intestinal nuclei (C, arrowheads) are in the same focal plane. (**D**) MLC migration in males. Male MLC leads extension into a final shape. Male DTCs do not lead arm extension. (**E** and **F**) MLC migration in wild-type (E) and *mig-17(K174)* (F) animals. Anterior is left and ventral is top. Bar, 20 μm.

when the MIG-17ΔDI protein was expressed in the DTCs using the *lag-2* promoter in *mig-17(k174)* mutants, it failed to rescue the DTC migration defects. In addition, a catalytically inactive MIG-17(E303A) and a MIG-17ΔPro lacking the pro-domain of MIG-17 were unable to localize on the surface of the gonad (Figs. 2B and 3, G through J). In contrast, the cysteine-rich domain is not required for the localization of MIG-17 on the gonad (Fig. 2B). Metalloprotease activity is therefore essential for the localization of MIG-17 on the gonad, and the DI domain may anchor MIG-17 to the gonad basement membrane.

DTCs migrate on a defined pathway while adhering to basement membrane during larval development. In *mig-17* mutants, the initial migration of DTCs along the ventral body wall muscles is normal, indicating that the MIG-17 metalloprotease is not required for DTC migration itself. However, subsequent dorsal migration is defective. Another set of *C. elegans* gene products, netrin UNC-6 and its receptors, UNC-5 and UNC-40, are critical for dorsal DTC migration, with UNC-6 acting as a guidance molecule in the basement membranes of the body wall and UNC-5 as a receptor for UNC-6 in the DTCs (*14*). We observed that introduction of *mig-17(k174)* enhanced the defect in dorsal DTC migration in *unc-6(e78)* mutants (Fig. 4D), suggesting that MIG-17 may be required for the processing or effecting of guidance cues provided by the UNC-5–UNC-6 system. For example, the MIG-17 metalloprotease may function in the basement membrane to modify the extracellular matrix, thus allowing the DTCs to attach to the body wall and be guided along the correct migration pathway. Another extracellular metalloprotease, GON-1, also controls DTC migration (*15*). Mutations in *gon-1* block DTC migration completely. GON-1 and MIG-17, although both metalloproteases, support different aspects of cell migration in *C. elegans* (*16*). Analysis of *C. elegans* metalloproteases should uncover structural changes in the extracellular matrix necessary for cell migration.

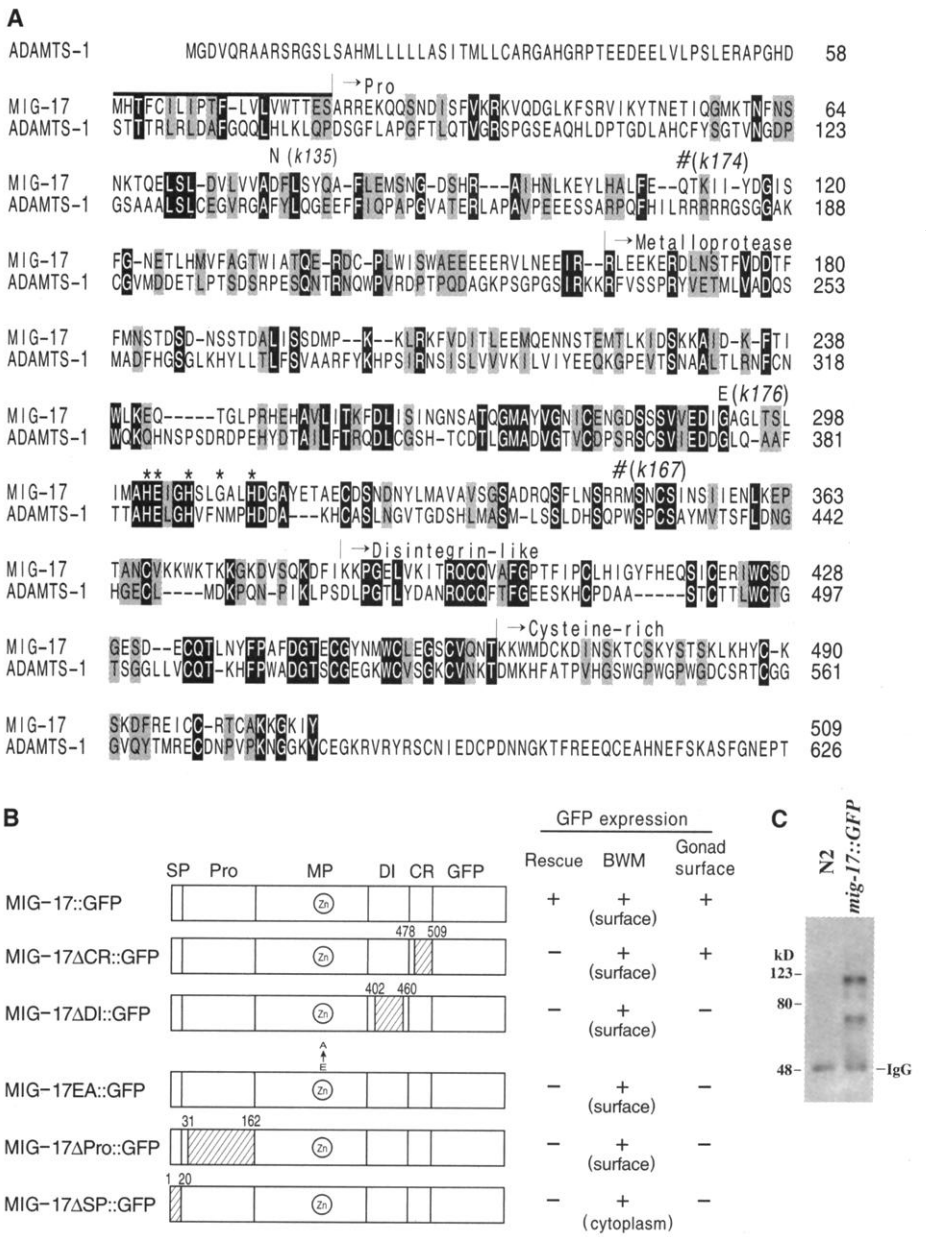

Fig. 2. The *mig-17* gene and protein. (**A**) MIG-17 sequence alignment with ADAMTS-1 (*8*). The COOH-terminal 325 amino acids of ADAMTS-1 are omitted. Black boxes, identical amino acids; gray boxes, similar amino acids; black bar, predicted signal peptide. In the metalloprotease domain, the zinc-binding motif (HEXXHXXGXXH) is marked by asterisks. The positions of *mig-17* mutations are indicated: D79N (GAC → AAC) in *k135*; Q111Stop (CAA → TAA) in *k174*; G292E (GGA → GAA) in *k176*; R347Stop (CGA → TGA) in *k167*. The accession number for the MIG-17 sequence is AB044562. (**B**) Domains of MIG-17. The transgenes are constructed as fusions with GFP. Hatched boxes show deleted regions. Each transgene was injected into *mig-17(k174)* and wild-type animals to test its ability to rescue DTC migration defects and its expression pattern, respectively. SP, signal peptide; MP, metalloprotease domain; DI, disintegrin-like domain; CR, cysteine-rich domain; BWM, body wall muscle. (**C**) Immunoblot analysis. Protein lysates from wild-type N2 or N2 expressing MIG-17::GFP were immunoprecipitated with anti-GFP and blotted with anti-GFP.

References and Notes

1. J. E. Kimble and J. G. White, *Dev. Biol.* **81**, 208 (1981); E. M. Hedgecock, J. G. Culotti, D. H. Hall, B. D. Stern, *Development* **100**, 365 (1987).
2. K. Nishiwaki, *Genetics* **152**, 985 (1999).
3. *Caenorhabditis elegans* hermaphrodites were observed using a Zeiss Axioplan microscope equipped with a Plan 100 objective and Nomarski differential interference contrast optics. Images were captured with a Hamamatsu Photonics C5810 Color Chilled 3-CCD Camera connected to a Macintosh G3 computer.
4. The *mig-17* gene was mapped to the right of the Bergerac *Tc1* polymorphism *bP1* on linkage group V by polymerase chain reaction–sequence tagged site (PCR-STS) mapping. Three-factor mapping placed *mig-17* between *bP1* and *daf-11*. Two cosmid clones, T26H10 and F57B7, were found to rescue *mig-17(k174)*. Four coding regions were predicted to lie within the region common to T26H10 and F57B7 by the *C. elegans* genome sequencing consortium computer analysis. The 5′ terminus of the *mig-17* message was analyzed using the 5′ RACE System (rapid amplification of cDNA ends; Life Technologies).
5. T. G. Wolfsberg and J. M. White, *Dev. Biol.* **180**, 389 (1996); P. Primakoff and D. G. Myles, *Trends Genet.* **16**, 83 (2000).
6. K. Kuno *et al.*, *J. Biol. Chem.* **272**, 556 (1997).
7. Mutants were isolated by ethylmethane sulfonate mutagenesis. The *mig-17* alleles *k135*, *k147*, *k167*, and *k176* were obtained by visual screening of mutants with ventral white-patch phenotypes.
8. Single-letter abbreviations for the amino acid residues are as follows: A, Ala; C, Cys; D, Asp; E, Glu; F,

Phe; G, Gly; H, His; I, Ile; K, Lys; L, Leu; M, Met; N, Asn; P, Pro; Q, Gln; R, Arg; S, Ser; T, Thr; V, Val; W, Trp; and Y, Tyr. X indicates any residue.

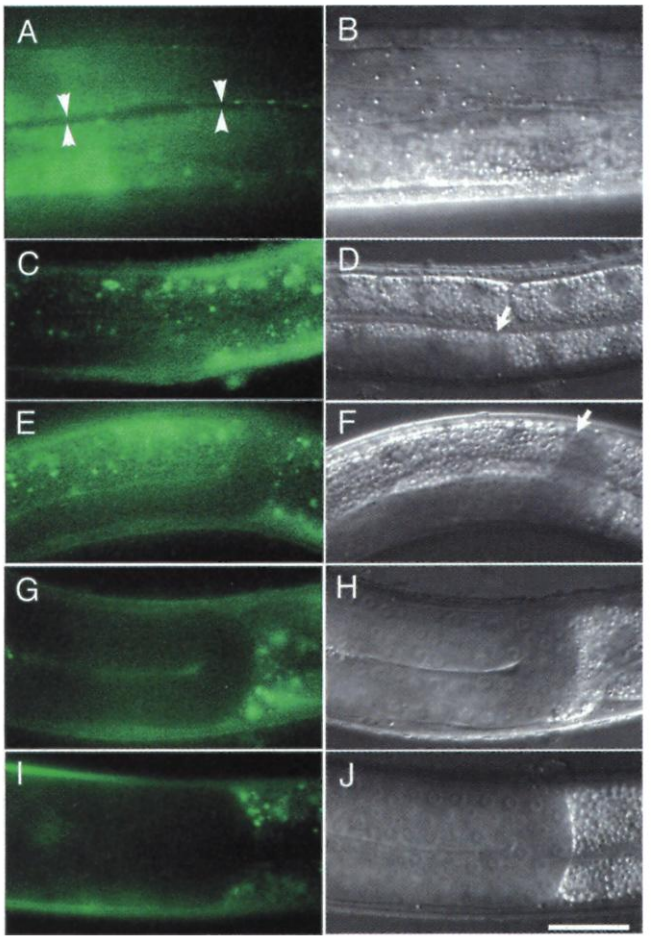

Fig. 3. Expression of *mig-17*. (**A**, **C**, **E**, **G**, and **I**) GFP fluorescence; (**B**, **D**, **F**, **H**, and **J**) Nomarski. Same animal in each left-right pair. Photos show ventral view (A and B) and lateral view of posterior gonad arms (C through J). (A through F) *mig-17(k174)* with *mig-17::GFP*; (G and H) *unc-119(e2498)* with *mig-17::GFP* and pDP#MM016B (*unc-119*); (I and J) *unc-119(e2498)* with *mig-17EA:GFP* and pDP#MM016B. (A and B) A young adult hermaphrodite. GFP is expressed on the pseudocoelomic face of ventral body wall muscles, but not on the ventral hypodermal ridge (arrowheads). (C and D) A mid L3 hermaphrodite. The DTC (arrow) starts turning dorsally. GFP is not expressed on the surface of gonad. The dotted fluorescence results from the auto-fluorescence of gut granules. (E and F) A late L3 hermaphrodite. The DTC migrates toward the dorsal muscle cells. GFP is expressed on the surface of gonad. [Frequency of GFP detection on the gonad: 0% (n = 12) during migration on ventral muscle; 44% (n = 9) during migration on lateral hypodermis; 90% (n = 21) during migration on dorsal muscle]. (G through J) Mid L4 hermaphrodites. MIG-17::GFP is expressed on the surface of the gonad, but MIG-17EA::GFP is not. Bar, 20 μm.

9. T. Crabbe *et al.*, *Biochemistry* **33**, 6684 (1994); J. Cha and D. S. Auld, *Biochemistry* **36**, 16019 (1997).
10. To construct the *mig-17::GFP* fusion, a 3645–base pair (bp) Sma I–Afl III *mig-17* fragment from the cosmid F57B7 was fused to a Bam HI–Spe I DNA fragment of the *GFP* plus *unc-54* 3′ untranslated region from pPD95.75 using appropriate synthetic oligonucleotides. This construct contained 1141 bp of the *mig-17* upstream sequence and the 2533-bp *mig-17* coding region and all introns. For constructions of *unc-54p::mig-17::GFP* and *lag-2p::mig-17::GFP*, the *mig-17::GFP* coding sequence was placed downstream of the *unc-54* promoter from pPD52.102 and the *lag-2* promoter from pRB1, respectively. Cosmid clones were co-injected at 10 to 50 μg/ml together with the pMK107 plasmid (100 μg/ml), which contains the EF1α promoter fused to GFP. Plasmid constructs were injected at 100 μg/ml with 50 μg/ml pBR322 either with or without 50 μg/ml *unc-119(+)* plasmid, pDP#MM016B [M. Maduro and D. Pilgrim, *Genetics* **141**, 977 (1995)].
11. Sonicated worm lysates were incubated with anti-GFP monoclonal antibody (Clontech) in a buffer containing 50 mM tris-HCl (pH 8.0), 100 mM NaCl, 10% glycerol, 1% Triton X-100, 5 mM phenylmethylsulfonyl fluoride, 1 μg/ml leupeptin, and 1 μg/ml pepstatin at 4°C for 3 hours. Samples were precipitated with protein A–Sepharose beads (Pharmacia). Immunoprecipitates were subjected to immunoblotting with anti-GFP antibody.
12. P. G. Okkema, S. W. Harrison, V. Plunger, A. Aryana, A. Fire, *Genetics* **135**, 385 (1993).
13. S. T. Henderson, D. Gao, E. J. Lambie, J. Kimble, *Development* **120**, 2913 (1994).
14. E. M. Hedgecock, J. G. Culotti, D. H. Hall, *Neuron* **4**, 61 (1990); C. Leung-Hagesteijn *et al.*, *Cell* **71**, 289 (1992); S. S.-Y. Chan *et al.*, *Cell* **87**, 187 (1996); W. G. Wadsworth, H. Bhatt, E. M. Hedgecock, *Neuron* **16**, 35 (1996).
15. R. Blelloch and J. Kimble, *Nature* **399**, 586 (1999); R. Blelloch *et al.*, *Dev. Biol.* **216**, 382 (1999).
16. In *mig-17(k174); gon-1(q518)* double mutants, DTCs did not migrate at all. In *mig-17(k174)/mig-17(k174); gon-1(q518)/+* animals, DTC migration defects of *mig-17(k174)* mutants were not enhanced.

17. We thank A. Coulson, A. Fire, J. Kimble, Y. Kohara, T. Stiernagle, and the Caenorhabditis Genetics Center for materials, and A. Antebi, E. Kipreos, M. Lamphier, and I. Mori for critical reading of the manuscript. Supported by special grants from PRESTO to K.N., and CREST, Uehara Memorial, and Advanced Research on Cancer from the Ministry of Education, Culture and Science of Japan to K.M.

30 December 1999; accepted 21 April 2000

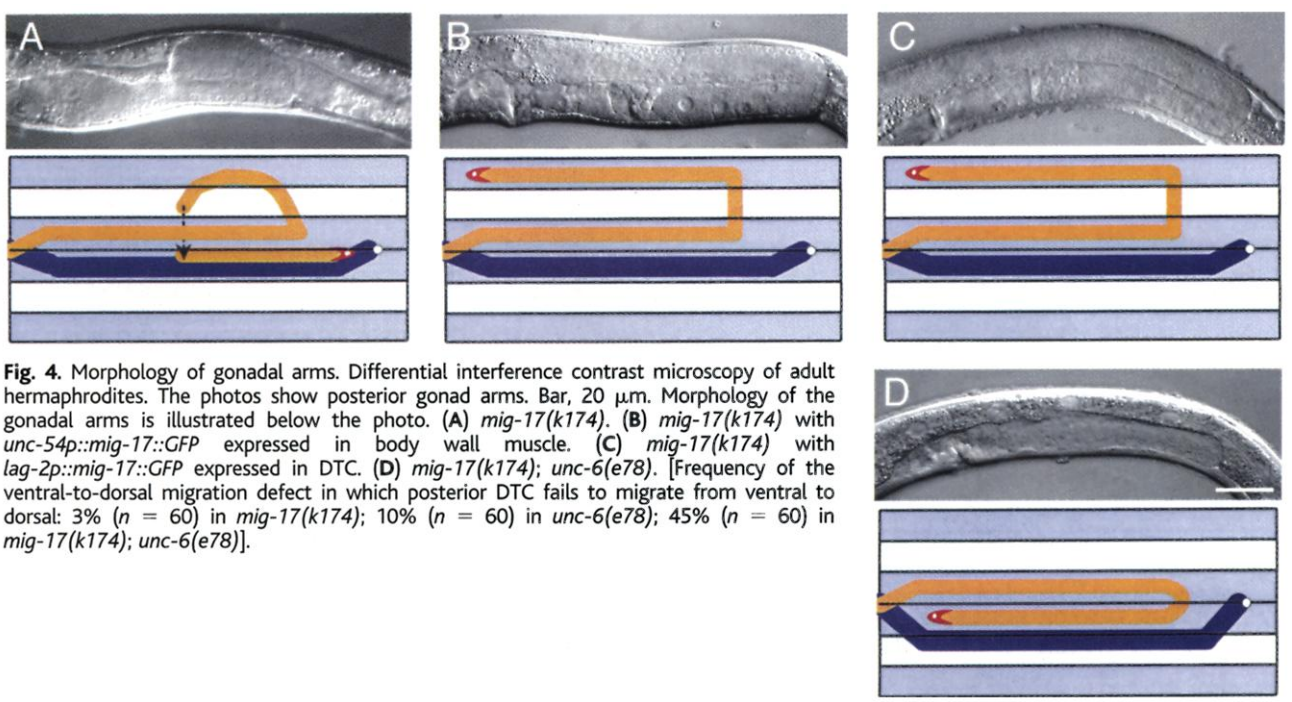

Fig. 4. Morphology of gonadal arms. Differential interference contrast microscopy of adult hermaphrodites. The photos show posterior gonad arms. Bar, 20 μm. Morphology of the gonadal arms is illustrated below the photo. (**A**) *mig-17(k174)*. (**B**) *mig-17(k174)* with *unc-54p::mig-17::GFP* expressed in body wall muscle. (**C**) *mig-17(k174)* with *lag-2p::mig-17::GFP* expressed in DTC. (**D**) *mig-17(k174); unc-6(e78)*. [Frequency of the ventral-to-dorsal migration defect in which posterior DTC fails to migrate from ventral to dorsal: 3% (n = 60) in *mig-17(k174)*; 10% (n = 60) in *unc-6(e78)*; 45% (n = 60) in *mig-17(k174); unc-6(e78)*].